Analytical and Bioanalytical Chemistry (2018) 410:6633–6642
https://doi.org/10.1007/s00216-018-1270-9

RESEARCH PAPER

Strong and oriented conjugation of nanobodies onto magnetosomes for the development of a rapid immunomagnetic assay for the environmental detection of tetrabromobisphenol-A

Jinxin He[1] · Jiesheng Tian[2] · Junjie Xu[2] · Kai Wang[1] · Ji Li[1] · Shirley J. Gee[3] · Bruce D. Hammock[3] · Qing X. Li[4] · Ting Xu[1]

Received: 22 May 2018 / Revised: 5 July 2018 / Accepted: 12 July 2018 / Published online: 1 August 2018

Abstract

Variable domain of heavy chain antibody (nanobody, Nb) derived from camelids is an efficient reagent in monitoring environmental contaminants. Oriented conjugates of Nbs and bacterial magnetic particles (BMPs) provide new tools for the high-throughput immunoassay techniques. An anti-tetrabromobisphenol-A (TBBPA) Nb genetically integrated with an extra cysteine residue at the C terminus was immobilized onto BMPs enclosed within the protein membrane, using a heterobifunctional reagent *N*-succinimidyl-3-(2-pyridyldithiol) propionate, to form a solid BMP-Nb complex. A rapid and sensitive enzyme-linked immunosorbent assay (ELISA) based on the combination of BMP-Nb and T5-horseradish peroxidase was developed for the analysis of TBBPA, with a total assay time of 30 min and a half-maximum signal inhibition concentration (IC_{50}) of 1.04 ng/mL in PBS (pH 10, 10% methanol and 0.137 moL/L NaCl). This assay can even be performed in 100% methanol, with an IC_{50} value of 44.3 ng/mL. This assay showed quantitative recoveries of TBBPA from spiked canal water (114–124%) and sediment (109–113%) samples at 1.0–10 ng/mL (or ng/g (dw)). TBBPA residues determined by this assay in real canal water samples were below the limit of detection (LOD) and in real sediments were between <LOD and 23.4 ng/g (dw). The BMP-Nb-based ELISA shows promising application in environmental monitoring.

Keywords Oriented conjugation · Nanobody · Bacterial magnetic particles · Immunomagnetic assay · Tetrabromobisphenol-A · Environmental detection

Introduction

Environmental management requires use of rapid and economical assays. Immunomagnetic assays refer to as identification and measurement of the target analytes via capture antibodies immobilized onto the surface of magnetic particles. The three-dimensionality and the high surface-area-to-volume ratio of the magnetic particles allow a relatively high probability of their interaction with targets, and consequently increase the assay efficiency in comparison with conventional enzyme-linked immunosorbent assays (ELISAs). The simple, rapid and innocuous nature of immunomagnetic assay techniques enables them widespread use in life and environmental sciences [1–3].

Magnetotactic bacteria, present in natural aquatic environments, are a group of gram-negative prokaryotes that biomineralize intracellular, lipid membrane-enclosed crystals of magnetic minerals called magnetosomes, also known as

Electronic supplementary material The online version of this article (https://doi.org/10.1007/s00216-018-1270-9) contains supplementary material, which is available to authorized users.

✉ Ting Xu
xuting@cau.edu.cn

[1] Beijing Advanced Innovation Center for Food Nutrition and Human Health, College of Resources and Environmental Sciences, China Agricultural University, No. 2 Yuan Ming Yuan West Road, Haidian District, Beijing 100193, China

[2] Department of Microbiology, College of Biological Sciences, China Agricultural University, Beijing 100193, China

[3] Department of Entomology and UCD Comprehensive Cancer Center, University of California, Davis, CA 95616, USA

[4] Department of Molecular Biosciences and Bioengineering, University of Hawaii at Manoa, 1955 East-West Road, Honolulu, HI 96822, USA

bacterial magnetic particles (BMPs) [4, 5]. BMPs are generally composed of single-domain ferrimagnetic iron oxide (magnetite, Fe_3O_4) or iron sulfide (greigite, Fe_3S_4) crystals which exist mainly in cub octahedral, elongated prismatic, and bullet-shaped morphologies [6]. BMPs have been studied for a wide variety of applications on the basis of their special characteristics such as nanoscale size (30–120 nm), dispersal ability, and membrane-bound structure [7]. An abundance of amino groups on the membrane of BMPs can be coupled to large quantities of bioactive substances such as antibodies [8–10], enzymes [4], antitumor drugs [11], and nucleic acids [12]. Since certain strains of magnetotactic bacteria can be fermented on a large scale, BMPs could provide economical and effective materials for immunomagnetic assays [13].

Antibodies linked to BMPs have higher activities than those immobilized onto synthesized magnetic particles [10, 14]. The coupling was achievable through the reaction between -NH_2 groups on the membrane of BMPs and -NH_2 or -SH groups of the antibodies in the presence of bifunctional reagents such as glutaraldehyde [11], carbodiimide [15], bis(sulfosuccinimidyl)suberate (BS_3) [16] and *N*-succinimidyl-3-(2-pyridyldithiol)propionate (SPDP) [17, 18]. Monoclonal antibodies (mAbs) were commonly applied to couple BMPs through their most reactive amine groups using glutaraldehyde or BS_3. However, this coupling may lead to the cross-link of the amine groups on the membrane and the random orientation of mAbs, so that a loss of recognition activity could happen [19]. Alternatively, an anti-*E. coli* mAb was immobilized onto BMPs in a site-directed way using a heterobifunctional reagent SPDP [17]. Nevertheless, reduction of antibodies was required in the presence of dithiothreitol which may reduce the antibody binding activity.

Advancements in the production of genetically engineered antibodies, including single-chain variable fragment (scFv) and variable domain of heavy chain antibody (VHH or nanobody (Nb)), over the last few decades have opened new avenues for the incorporation of functionalities and tags for numerous applications, such as detection, purification, conjugation and immobilization purposes [20, 21]. Camelid Nbs are well known having a number of advantages such as small size, high solubility, high thermal stability and cost-effective production. They were genetically modified for bioanalytical applications, e.g., as capture reagents in biosensors and affinity chromatography [22, 23]. In a Nb-based diagnostic study, Nbs specific for carcinoembryonic antigen (CEA) were tagged with quantum dots through an additional cysteine (Cys) residue integrated within the C terminus of the nanobodies, allowing for the excellent specificity of flow cytometry quantitative discrimination of CEA positive and negative tumor cells [24]. Combination of Nbs and BMPs in biotechnological application was scarce and limited to a study on magnetosome-specific expression of a red fluorescent protein (RFP)-binding Nb in vivo, accomplished by genetic fusion of Nb to the magnetosome protein MamC in magnetotactic bacteria [25]. The isolated magnetosomes expressing MamC-Nb was used for immunoprecipitation of RFP-tagged proteins and their interaction partners from cell extracts.

Owing to the easy manipulation of both BMPs and Nbs, combined use of these materials might provide a valuable tool for monitoring environmental chemicals. As a proof of concept, in the present study, we developed a small, stable, and specific BMPs with oriented conjugation of Nbs for the rapid and sensitive detection of tetrabromobisphenol-A (TBBPA) in water and sediments. TBBPA is a currently intensively used brominated flame retardant showing widespread environmental and human exposures. Due to its high lipophilicity and persistence, TBBPA could be detected in wastewater [26], fresh surface water [27, 28] and sediments [29].

Material and methods

Chemicals and reagents

The TBBPA standard was purchased from TCI Co., Ltd. (Tokyo, Japan). Ring-$^{13}C_{12}$ labeled TBBPA (99% purity) was obtained from Cambridge Isotope Laboratories, Inc. (Andover, MA). Isopropyl-β-D-thiogalactopyranoside (IPTG), 3,3′,5,5′-tetramethylbenzidine (TMB), *p*-nitrophenyl phosphate (pNPP), imidazole, alkaline phosphatase (AP), horseradish peroxidase (HRP) and SPDP were purchased from Sigma-Aldrich Chemical Co. (St. Louis, MO, USA). All restriction enzymes and T4 DNA ligase were purchased from New England Biolabs, Inc. (Ipswich, MA). HisPur Ni-NTA resin, Halt protease inhibitor cocktail, and Nunc MaxiSorp flat-bottom 96-well plates were purchased from Thermo Fisher Scientific Inc. (Rockford, IL). Competent cell *E. coli* DH5α and pClone007 Simple Vector were purchased from Tsingke Biological Technology Lt. (Beijing, China).

Preparation of BMPs

BMPs were isolated from bacteria *Magnetospirillum gryphiswaldense* strain MSR-1 (DSM 6361) and then purified according to the methods described previously with slight modification [16]. Briefly, approximately 10 g bacteria suspended in 200 mL of phosphate buffered saline (PBS, 0.01 moL/L phosphate, 0.137 moL/L NaCl, and 0.003 moL/L KCl, pH 7.4) were disrupted by sonication for 25 min (10 s each, 50 cycles with 5 s interval) at 200 W. Afterwards, the suspension of BMPs was magnetically separated by using a strong magnet and then the supernatant was removed. The separated BMPs were re-suspended in PBS and sonicated for 15 min at 3 s/time with the interval of 5 s at 120 W to lyse MSR-1 cells. The suspension was placed on the magnet to separate the BMPs. The procedure was repeated twice with

the power changing to 80 and 40 W, respectively, until the concentration of supernatant protein was less than 0.1 ng/mL. After washing with PBS buffer five times, BMPs were collected and kept at − 70 °C until use. The purity and size of BMPs were assessed by transmission electron microscopy (TEM) (JEM-1400, Japan; CCD: Gatan 832, 4 k × 3.7 k, USA). The hydrated radii, zeta potentials and polydispersity of BMPs were analyzed by a zeta potential analyzer (Brookhaven Instruments Corp., Long Island, NY).

Construction of recombinant plasmid and expression of Nb-Cys

The anti-TBBPA Nb (T3–15) was isolated from an immunized alpaca library as previously described [30]. The primers 5′-C*AAGCTT*CAGTTGCAGCTCGTGGAGTC-3′ and 5′-CC*GAGCTC*TCAACAATGTGATGGTGATGATGGTC TTG-3′, including *Hind III* and *Xho I* restriction site underlined, were used to clone the target Nb gene, and an extra C-terminal cysteine residue following 6 × His tag was introduced simultaneously, yielding a Nb-6His-Cys fragment. After purification, the fragment was cloned into a pClone007 Simple Vector and transformed into the competent cell *E. coli* DH5α. After sequence, the target fragments were cloned into pET29a digested by the same enzymes, resulting in recombinant plasmids pET29a-Nb-Cys, and introduced into *E. coli* BL21(DE3)pLysS. A single positive colony was cultured at 37 °C in 1 L of Luria-Bertani (LB) liquid medium supplemented with kanamycin (50 μg/mL) until the OD_{600} reached 0.5, and then induced by adding IPTG at a final concentration of 1.0 mmoL/L for 8 h. After harvesting the cells by centrifugation (8000×*g*, 15 min, 4 °C), the pellets were lysed by sonication (10 s each, 10 cycles with 5 s interval) in ice water bath. After another centrifugation (10,000×*g*), the supernatant of lysate was collected. Proteins were purified with a Ni-NTA column. The purity and size of proteins were analyzed on 12% sodium dodecyl sulfate polyacrylamide gel electrophoresis (SDS-PAGE).

Oriented immobilization of Nbs onto BMPs

An aliquot of 2.5 μL of SPDP dissolved in dimethyl formamide (1 mM) was added to 1 mL of BMPs suspension (10 mg/mL) in PBS (pH 7.4). The suspension was then dispersed by sonication and incubated for 2 h at room temperature. The SPDP-modified BMPs were washed with PBS for three times and then incubated with Nb-Cys solution for 2 h at room temperature. The concentration of Nb-Cys in the solution was evaluated by using a BCA protein assay kit (Pierce, Rockford, IL) before and after immobilization, and the quantities of Nb-Cys immobilized on BMPs were calculated. The constructed BMP-Nb complexes were washed three times with PBS (pH 8.0) to remove nonspecifically adsorbed antibodies. BMP-Nb was identified by a Western blotting analysis. The bands of BMP-Nb complexes on a SDS-PAGE gel were transferred onto a nitrocellulose membrane by electroblotting and blocked with 1% BSA overnight at 4 °C. Diluted mouse anti-His mAb was used as primary antibody (1:25,000, *v*/*v*) incubated with the membrane under gentle agitation for 1 h at room temperature. The membrane was rinsed to remove unbound primary mAb and then placed in a solution of secondary antibody (goat anti-mouse IgG labled with AP) for 1 h at room temperature. After washing three times with PBST (PBS containing 0.05% Tween-20), the reactivity was detected by 5-bromo-4-chloro-3-indolyl phosphate and nitro blue tetrazolium to generate a precipitate in proportion to the amount of protein.

To optimize the linkage of Nb-Cys to BMPs, a variable quantity of Nb-Cys (0.2, 0.5, 1.0, and 1.2 mg) was mixed with 1 mg SPDP-modified BMPs in 1 mL of PBS and incubated for different time (30, 60, 90, 120, and 150 min). The Nb-Cys concentration in the solution before and after reaction was measured and the linkage rate was calculated as the method reported by Li et al. [16].

Coupling TBBPA derivatives to enzymes

TBBPA haptens T3 and T5 (see Electronic Supplementary Material (ESM) Fig. S1) available from our previous study [31] were coupled to HRP and AP according to the method reported by Schneider and Hammock [32]. The concentrations of hapten-enzyme conjugates, termed as tracers, were determined by the BCA protein assay.

BMP-Nb-based ELISA for TBBPA

A 96-well microtiter plate was blocked with 1% gelatin (300 μL per well) in carbonate-bicarbonate buffer (pH 9.6) at 4 °C overnight and washed with PBST. The BMP-Nb complexes were blocked with 1% gelatin overnight and the BMP-Nb suspension was added to the blocked plate above (100 μL per well). This plate was fastened to a 96-well magnetic frame and washed three times with PBST. Two assay formats, defined as one- and two-step, were conducted for the detection of TBBPA. For one-step, an aliquot of TBBPA and tracer in PBS (each 50 μL) was added to the well holding BMP-Nb and the mixture was incubated on an oscillator (150 rpm/min) for 30 min without magnet. The plate was washed three times with PBST as above. For two-step, 50 μL of TBBPA solution was added to the well with BMP-Nb and incubated for 10 min, followed by the addition of 50 μL of tracer. After another 5 min incubation, the plate was washed. For AP and HRP activity, 150 μL of 1.0 mg/mL pNPP (1 M glycine buffer, 1 mM $MgCl_2$, and 1 mM $ZnCl_2$, pH 10.4) and 100 μL of TMB solution (400 μL of 0.6% TMB and 100 μL of 1% H_2O_2 dilution in 25 mL of citrate buffer, pH 5.5) were added

into the plate, and the reaction was stopped 8 min later by the addition of 50 μL of 3 M NaOH and 2 M H_2SO_4, respectively. The absorbance was read at 405 and 450 nm on a microtiter plate reader (ELx800, BioTek, USA) for AP and HRP, respectively. The half-maximum signal inhibition concentration (IC_{50}), an indicator of the assay sensitivity, and the limit of detection (LOD), denoted as IC_{10}, were obtained from a four-parameter logistic equation generated by SigmaPlot 10.

Effects of pH, organic solvent, and ionic strength on ELISA

To evaluate the effects of physicochemical factors on ELISA (maximal signal A_0 and IC_{50}), this assay was performed in PBS with various pH (3.0–11.0), different concentrations of methanol (MeOH) (5–100%, *v*/*v*) and different concentrations NaCl (0–2.188 moL/L). Except for the single variable, pH 10, 0.137 moL/L NaCl, 0.003 moL/L KCl, and 10% MeOH.

Sample analysis and validation

Water and sediment samples were collected from the Xiao Qing He canal in Beijing, China. Sediments were lyophilized, ground, and sieved through a 20-mesh (0.9 mm aperture) screen. Blank water and sediment samples free of TBBPA identified by a liquid chromatography tandem mass spectrometry (LC-MS/MS) were used for the recovery study. Water samples were fortified with TBBPA at final concentrations of 1.0, 5.0, and 10 ng/mL. After passing through a 0.22-μm filter (Waters, MA, USA), water samples were diluted at least 4-fold with PBS (pH 10, 10% MeOH) and subjected to BMP-Nb-based ELISA. A dry weight (dw) of 1.0 g sediment was weighed in a 50-mL glass tube and spiked with TBBPA (1.0, 5.0, and 10 ng/g (dw)). The samples were extracted twice with 10 mL of methanol/acetone (50:50, *v*/*v*) (× 2) in an ultrasonic water bath for 15 min at room temperature. The slurry was centrifuged at 8000×*g* for 10 min to collect the supernatant. The combined supernatant was evaporated to near dryness under a gentle stream of nitrogen and the residue was redissolved in 200 μL of methanol. The extracts were diluted with PBS at least 20-fold prior to ELISA. The ELISA results were finally validated with a LC-MS/MS method described by Yang et al. [33].

Results and discussion

Preparation of BMPs

The BMP production in magnetotactic bacteria was observed under aerobic and strict anaerobic conditions, with yield in the following order of *M. gryphiswaldense* strain MSR-1 > *M. magneticum* strain AMB-1 > *M. magnetotacticum* strain MS-1 after 24 h of fermentation [34]. MSR-1, a kind of magnetic Spirillum, was thereby selected to produce BMPs with the medium and culturing conditions optimized by Zhang et al. [35, 36]. The yield of BMPs (Fe_3O_4) reached to 402 mg/L by dry weight after 48 h of fermentation, showing a cost-effective production. TEM image of 500 BMPs revealed that most of the BMPs have a narrow size distribution of 20–50 nm in diameter (Fig. 1A and C). Although the average hydrated radius of BMPs was 282.4 nm, their zeta potentials were lower than − 30 mV (see ESM Table S1), illustrating that the aqueous colloids were quite stable. Mass production of BMPs would facilitate their detailed biotechnological applications.

Construction of Nb-Cys

The alpaca-derived Nb T3–15 has demonstrated high selectivity and sensitivity to TBBPA [30, 37]. In the analysis of amino acid sequences of the Nb, only one pair of intrinsic cysteines was found which may form a disulfide bond to maintain the structure stability (Fig. 2A), hardly providing any free sulfhydryl groups for reaction with SPDP. Reduction of the Nb may alter its structure and binding affinity and thus was avoided. It was reported that the functional parts of Nbs are closely located at N terminus of their three-dimensional structures [38]. Therefore, the Nb was C-terminally fused to a 6 × His tag for purification purpose, followed by an additional single free cysteine residue for specific reaction with SPDP (Fig. 2A). After expression and purification, the protein was analyzed on a SDS-PAGE gel and a prominent band with the expected size (~ 15 kD) was observed (Fig. 2B), indicating the emergence of the protein Nb-Cys. The yield of Nb-Cys was approximately 30 mg from 1 L bacterial culture media.

Oriented conjugation of Nb onto BMP

SPDP is a short-chain crosslinker for amino-to-sulfhydryl conjugation via N-hydroxysuccinimide ester and pyridyldithiol reactive groups to form a peptide bond and a cleavable (reducible) disulfide bond, respectively [39]. In the section above, the specific integration of a single cysteine residue at the C terminus of the Nb amino acid sequence was done to facilitate the oriented conjugation with BMPs. The linking efficiency of Nb-Cys to SPDP-modified or non-modified BMPs was evaluated and meanwhile, the parental Nb was used as a control. For the SPDP-modified BMPs, linkage rate from the incubation of Nb-Cys/BMP was much higher than that of Nb/BMP (Fig. 3A and B), indicating the specific reaction between SPDP and Nb-Cys, and the weak reaction between SPDP and the parental Nb (linkage rate < 8%). For the non-modified BMPs, nonspecific adsorption rates of Nb-Cys and Nb on BMPs in the absence of SPDP were below 5% (Fig. 3C and D). The maximum linkage rate of

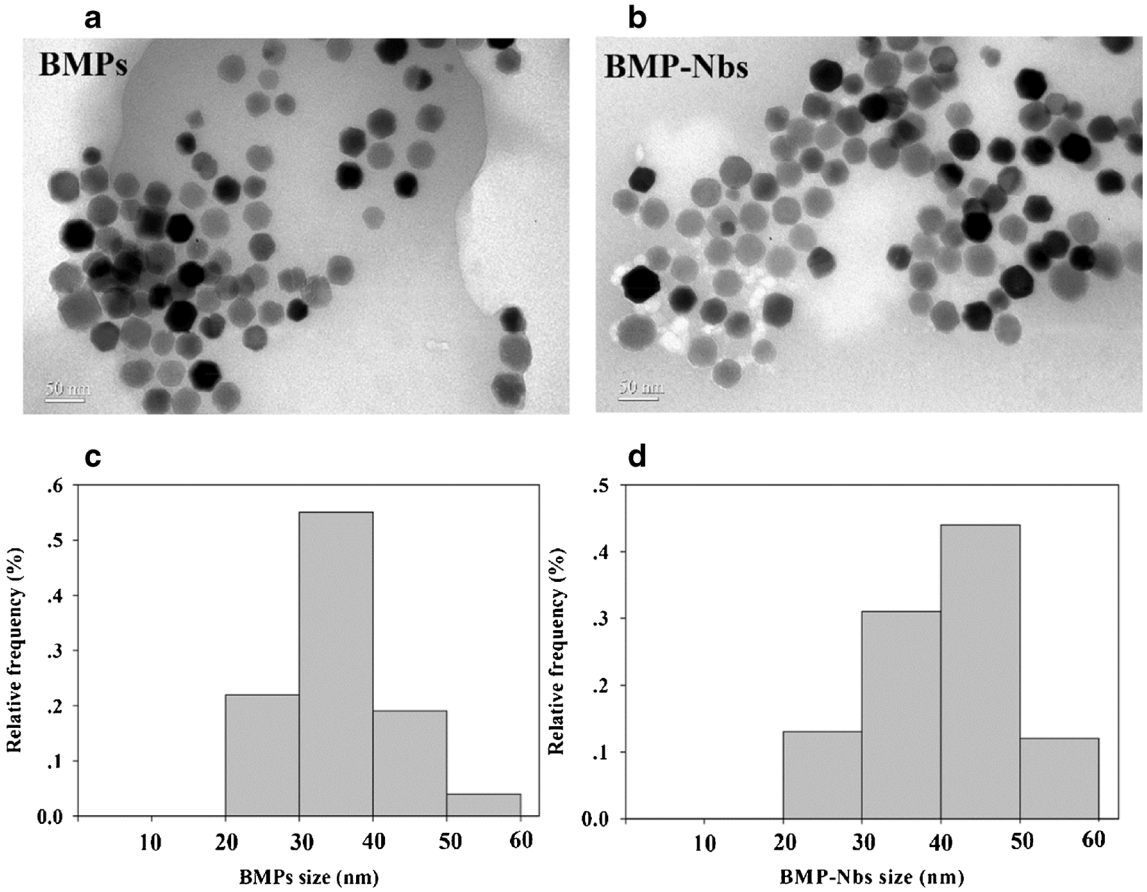

Fig. 1 TEM images of particle BMPs (**A**) and BMP-Nbs (**B**). Particle size distribution of BMPs (**C**) and BMP-Nbs (**D**). A total of 500 BMPs or BMP-Nbs were measured

81% (810 μg/mg) was achieved by mixing Nb-Cys and BMPs each at a final concentration of 1 mg/mL (see ESM Fig. S2, A), and incubating for 120 min (see ESM Fig. S2, B). The constructed complex of BMP-Nb was confirmed by Western blotting analysis, as an obvious reaction occurred at MW ~ 15 kD (Fig. 3, inset). BMP-Nbs were associated with higher values of hydrated radii, zeta potential and polydispersity than BMPs (see ESM Table S1), but the size distribution of BMP-Nbs was similar to that of BMPs (Fig. 1B and D). The low zeta potential of BMP-Nbs (− 46.86 mV) indicated that a stable aqueous colloid solution of BMP-Nbs was obtained.

Binding activity of BMP-Nb to tracers

AP and HRP have demonstrated advantages of high stability, high activity and cost-effectiveness in ELISAs and thereby

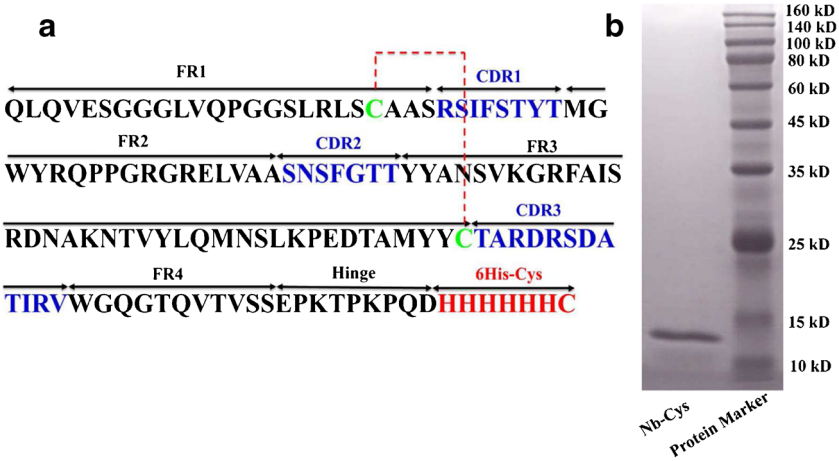

Fig. 2 The amino acid sequences of modified Nb and identification of Nb-Cys. (**A**) The Nb was C-terminally fused to a 6 × His tag, followed by an additional single free cysteine residue (red). The red dash line indicates possible formation of the disulfide bond. (**B**) SDS-PAGE image of Nb-Cys

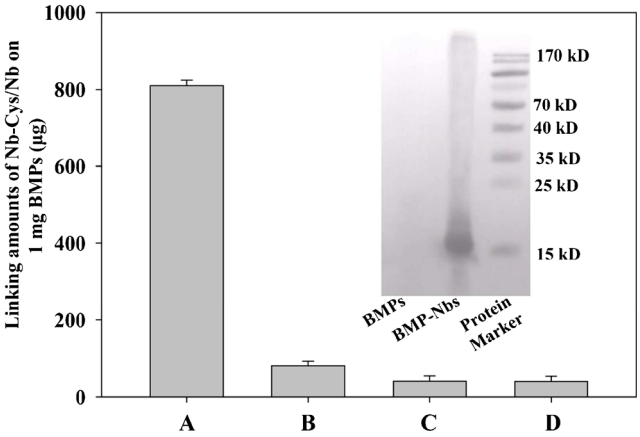

Fig. 3 Coupling of Nb-Cys/Nb to SPDP-modified or non-modified BMPs. (**A**) Nb-Cys with SPDP-modified BMPs. (**B**) Nb with SPDP-modified BMPs. (**C**) Nb-Cys with non-modified BMPs. (**D**) Nb with non-modified BMPs. The data are the average of triplicates. The inset is the Western blotting image for identification of BMP-Nb

were employed to label haptens in the present study. The binding affinity of BMP-Nb to tracers was evaluated by a competitive immunomagnetic assay in the presence of TBBPA (100 ng/mL) (Fig. 4). BMP-Nb demonstrated higher binding affinity to T5-AP/HRP than to T3-AP/HRP, which was expected since the anti-TBBPA Nb was generated from the immunogen T5-thyroglobulin [30]. Additionally, higher binding activity and inhibition by TBBPA were observed from the combination of BMP-Nb and T3/T5-HRP (Fig. 4A) than that of BMP-Nb and T3/T5-AP (Fig. 4B). A possible reason was that AP (112 kD) caused a stronger steric hindrance than HRP (44 kD), due to the size difference. Another was that tracer construction may somewhat lead to the loss of AP activity. In terms of hapten disparity, higher sensitivity was obtained from combination of BMP-Nb/T5-HRP than from that of BMP-Nb/T3-HRP, reverse to the outcomes of linker length effect on the traditional ELISA [31]. Since BMP-Nb exhibited satisfactory binding activity to both T5-HRP and TBBPA, the combination of BMP-Nb/T5-HRP was selected for the development of an immunomagnetic assay for TBBPA.

Optimization of BMP-Nb-based ELISA for TBBPA

BMPs were reported to possess intrinsic peroxidase-like activity [40] which could interfere with the activity of tracer hapten-HRP employed in the BMP-Nb-based ELISA. Generally, signal detection of BMP-based immunoassays was related to AP tracer or fluorescent tracer [25, 41]. In an attempt to develop a BMP-Nb/T5-HRP-based assay, it is essential to adjust the concentration of BMP-Nb to a threshold suitable for detection purpose and elimination of the peroxidase-like activity of BMP. Thus, various amount of BMP-Nb in TMB solution (100 μL per well) was incubated for 30 min at room temperature and then the absorbance was detected. It was noteworthy that the peroxidase-like activity was reduced when BMPs were coupled with Nbs (see ESM Fig. S3). As the concentration of BMP-Nb was below 1.0 mg/mL, low OD_{450} (< 0.1) was observed (see ESM Fig. S3), indicating the elimination of enzyme mimetic activity. As determined by a checkerboard method, 160 μg/mL BMP-Nb/PBS suspension (100 μL per well) and 22 ng/mL T5-HRP (50 μL per well) were selected for the next assay optimization.

In order to optimize the BMP-Nb-based assay, one- and two-step assays were evaluated by comparing their sensitivities and performance time. The IC_{50} values of one- and two-step assays were 50.9 and 6.48 ng/mL, respectively (see ESM Fig. S4, A). The sensitivity difference may result from the different binding priority of Nb to targets. In one-step format,

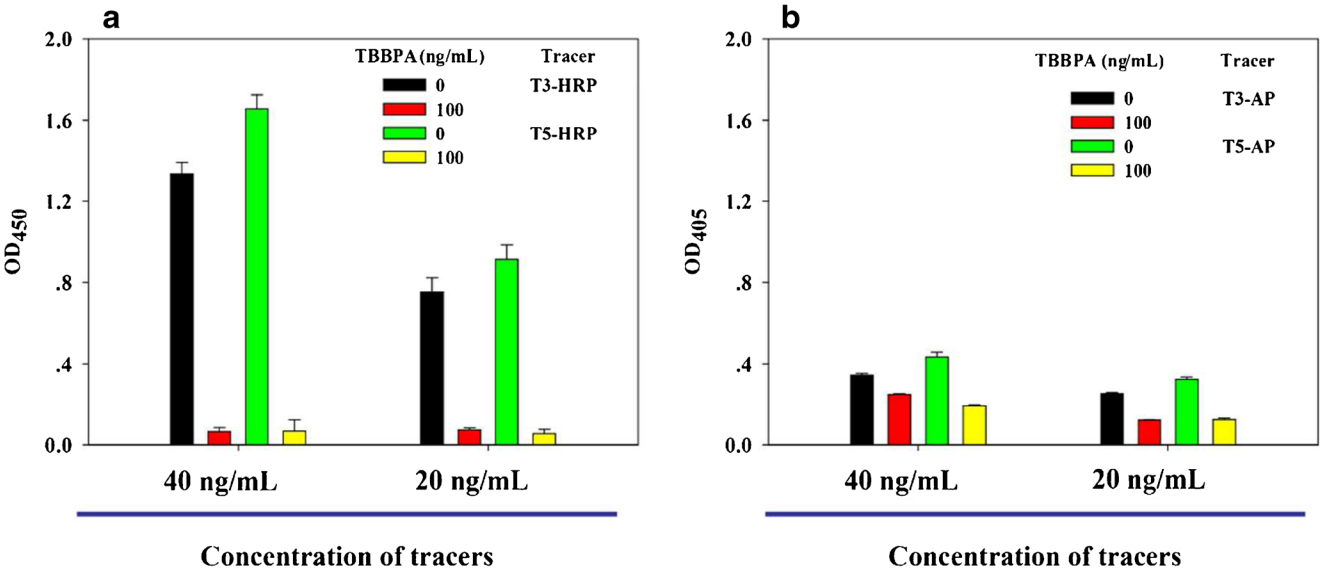

Fig. 4 Binding activity of BMP-Nb to tracers T3/T5-HRP (**A**) and T3/T5-AP (**B**) in the presence or absence of TBBPA; the concentration of BMP-Nb/PBS suspension was 150 μg/mL

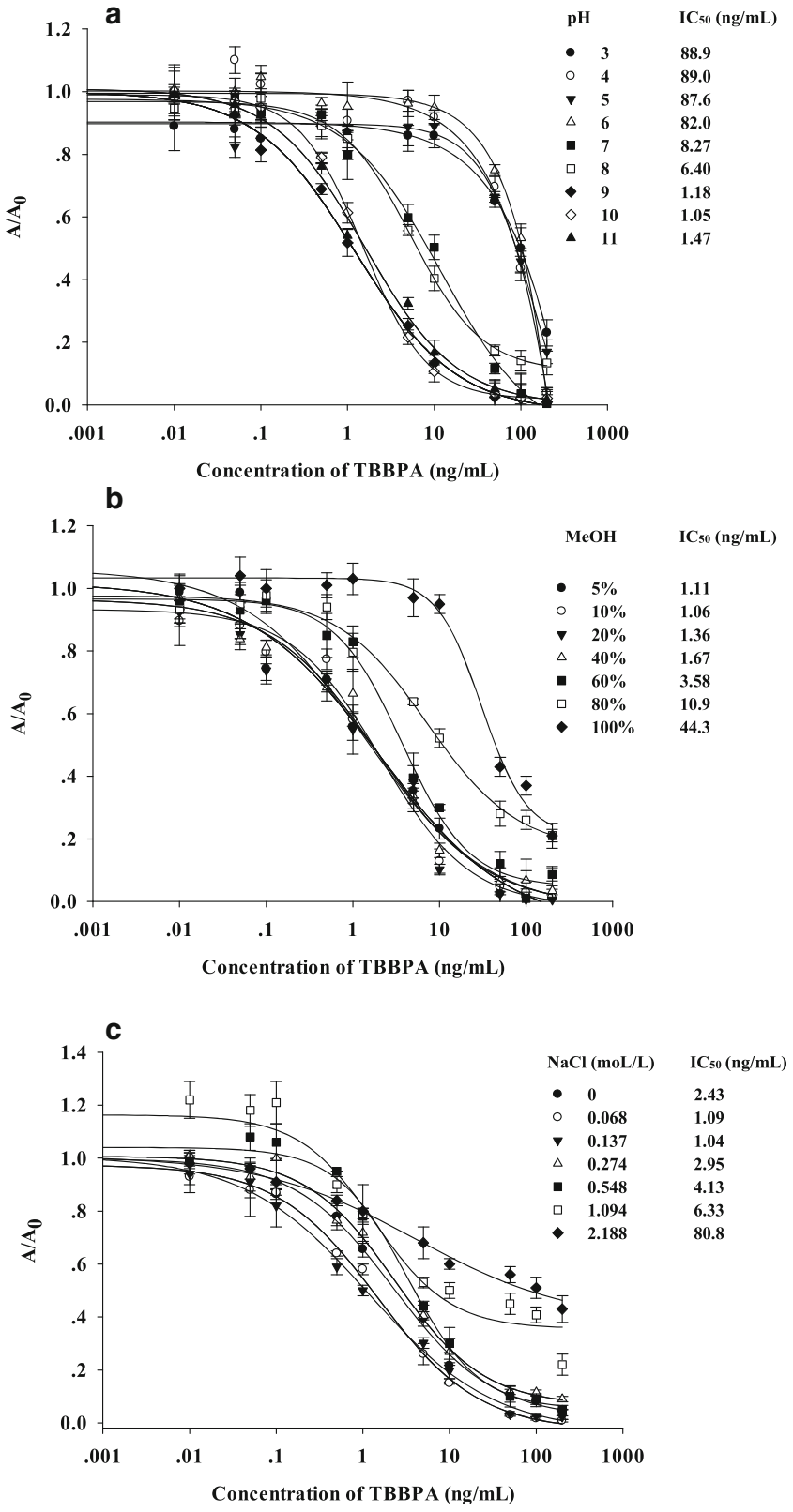

Fig. 5 Effects of pH (**A**), MeOH (**B**), and NaCl (**C**) on the performance of BMP-Nb-based ELISA for TBBPA at ambient temperature. Except for the single variable, pH 10, 0.137 moL/L NaCl, 0.003 moL/L KCl, and 10% MeOH. The data shown are the average of triplicates

TBBPA and T5-HRP shared the equivalent opportunities binding to Nb, whereas, in two-step format, the binding sites of Nb were occupied by TBBPA in the first step and provided few spaces for tracers in the second step, consequently improving the assay sensitivity.

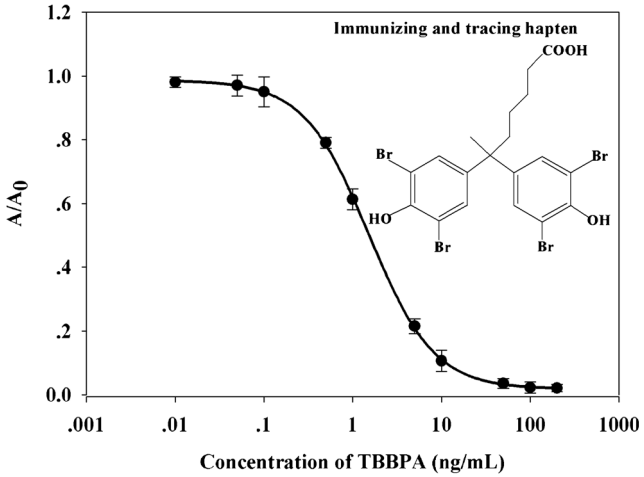

Fig. 6 Calibration curve of BMP-Nb-based ELISA for TBBPA. Each value is the average of four replicates and the standard deviations

Compared to one-step assay, two-step assay is more complicated but showed higher sensitivity required for the detection of low level of TBBPA in the environment. The two-step format was selected for the remainder of this study and the incubation time of each step was optimized. In the first step, it took approximately 10 min for the reaction of BMP-Nb with TBBPA (5 ng/mL) to reach to a balance (see ESM Fig. S4, B, Curve-1). In the second step, the competition between T5-HRP and TBBPA for the binding sites of BMP-Nbs could achieve a balance in about 5 min (see ESM Fig. S4, B, Curve-2). Thus, for the BMP-Nb-based competitive ELISA, the incubation time for the first step and the second step was 10 and 5 min, respectively.

Effect of physicochemical property on ELISA

The effect of buffer pH on the BMP-Nb ELISA was evaluated firstly and this assay had a higher sensitivity in basic buffer than in acidic one, with the least IC_{50} of 1.05 ng/mL at pH 10 (Fig. 5A). It is possible that the basic condition could stabilize BMP-Nb and increase TBBPA solubility in buffer [42]. Thus, the following immunoassays were conducted in PBS (pH 10). Although anti-TBBPA Nb has shown strong tolerance to MeOH in our previous report [30, 37], the influence of the organic solvent on BMP-Nb-based ELISA remained unknown and should be evaluated prior to the application in real environmental samples. As shown in Fig. 5B, IC_{50} and A_0 values ranged from 1.06 to 44.3 ng/mL and from 0.893 to 0.924, respectively, with the increase of MeOH from 5 to 100%. Slight change of BMP-Nb binding to TBBPA was observed with MeOH in a range of 5–40% and the most sensitive assay (IC_{50}, 1.06 ng/mL) was obtained at 10% MeOH, with a reasonable A_0 (0.924) (Fig. 5B). This high resilience to MeOH could be explained that the short time (10 min) exposure of BMP-Nb in 100% organic solvent did not totally denature either BMP membrane protein or Nb. Thus, MeOH was qualified to stabilize TBBPA for the BMP-Nb-based competitive ELISA, and 10% MeOH was selected for the remainder of this study. As NaCl concentration increased from 0 to 2.188 moL/L, the IC_{50} and A_0 varied in a range of 1.04–80.8 ng/mL and 0.934–0.534, respectively (Fig. 5C). Strong ionic strength might interfere with the interaction between antibody and analyte, resulting in the decline of assay signal and sensitivity. In the current assay, 0.137 moL/L NaCl in PBS was selected because the satisfactory A_0 (0.916) and IC_{50} (1.04 ng/mL) values were exhibited under this ionic strength.

The typical calibration curve of BMP-Nb-based ELISA for TBBPA was generated in PBS (pH 10) containing 10% MeOH and 0.137 moL/L NaCl (Fig. 6). This assay had a linear range of 0.45–5.25 ng/mL (IC_{20}–IC_{80}), an IC_{50} value of 1.04 ng/mL, and a LOD of 0.1 ng/mL, which are comparable to those of traditional Nb-based ELISAs reported previously [30].

Sample analysis

Matrix effect is inevitable in sample extract and easy to cause false positive results in immunoassays. Dilution of extract is

Table 1 Determination of TBBPA spiked in water and sediments by ELISA and LC-MS/MS

Samples	Spiked level in water (ng/mL) and sediment (ng/g (dw))	Average recovery (%) ± CV ($n = 3$)*	
		ELISA	LC-MS/MS
Canal water	0	ND	ND
	1.0	118 ± 5.5a	95 ± 2.2a
	5.0	114 ± 4.8a	117 ± 3.9a
	10	124 ± 6.4a	106 ± 1.9a
Canal sediment	0	ND	ND
	1.0	113 ± 3.2a	91 ± 3.7a
	5.0	109 ± 2. 2a	95 ± 3.6a
	10	112 ± 4.7a	87 ± 4.6b

*Different letters following the means ± CV in a row indicate a significant difference by ANOVA, $P < 0.05$. ND, not detectable

an effective strategy to eliminate the matrix effect, whereas, this method will lead to a loss of assay sensitivity. For the developed immunomagnetic assay, a 4-fold and a 20-fold dilution with PBS (pH 10) containing 10% MeOH for water and sediment extract, respectively, were qualified to eliminate the matrix effect (see ESM Fig. S5) and enable the detection of TBBPA at low level (see Table 1). The recoveries of TBBPA from water and sediment samples by the BMP-Nb-based ELISA were in a range of 114–124% and 109–113%, respectively (see Table 1). This assay was validated by comparing the recoveries with those of an instrumental method LC-MS/MS, by which recoveries were in a range of 87-117% (see Table 1). Both methods showed good recoveries and correlated well with each other (see ESM Fig. S6). Difference between two analysis methods for TBBPA was tested by the one-way ANOVA in the SPSS software package (20.0, USA). A significant difference was only observed from the analyses of sediments spiked with 10 ng/g (dw) TBBPA ($p < 0.05$) (see Table 1). The ELISA method was also applied to analyze TBBPA in real world samples including 5 waters and 7 sediments collected in the Xiao Qing He canal, Beijing. The levels of TBBPA by ELISA were below the LOD in all water samples but detectable in three sediments (6.21, 9.56 and 23.4 ng/g (dw)), in agreement with those from LC-MS/MS (see ESM Table S2). Therefore, the developed immunomagnetic assay was demonstrated to be a valid method to detect TBBPA in water and sediments.

Conclusion

For the first time, an immunomagnetic assay for the detection of TBBPA in water and sediments using the combination of BMP-Nb and tracer hapten-HRP was developed. The anti-TBBPA Nb modified by fusing a cysteine at the C terminus allows for the ready site-directed conjugation to BMPs in the presence of a linkage reagent SPDP. Compared to the previous Nb study [30], the BMP-Nb-based ELISA is little less sensitive to TBBPA, with IC_{50} values of 1.04 ng/mL vs 0.4 ng/mL, but needs shorter assay time, approximately 0.5 vs 2.5 h. Moreover, this assay showed high resilience to MeOH in a range of 5–40%. The results of the BMP-Nb-based ELISA for TBBPA in environmental samples were correlated well with those from LC-MS/MS. The easy availability and cost-effectiveness of BMP-Nb complexes make them attractive as a tool in the environmental monitoring and the commercial application of these materials may be expected in the near future.

Acknowledgements This work was supported in part by the Project of the National Natural Science Foundation of China (21577170), Key Project of Inter-Governmental International Scientific and Technological Innovation Cooperation (2016YFE0108900), China and the National Institute of Environmental Health Sciences Superfund Research Program, P42ES04699, USA.

Compliance with ethical standards

The authors declare that they have no conflict of interest. This research did not involve human participants or animals.

References

1. Orlov AV, Bragina VA, Nikitin MP, Nikitin PI. Rapid dry-reagent immunomagnetic biosensing platform based on volumetric detection of nanoparticles on 3D structures. Biosens Bioelectron. 2016;79:423–39.
2. Deng Q, Qiu M, Wang Y, Lv P, Wu C, Sun L, et al. A sensitive and validated immunomagnetic-bead based enzyme-linked immunosorbent assay for analyzing total T-2 (free and modified) toxins in shrimp tissues. Ecotoxicol Environ Saf. 2017;142:441–47.
3. Felix FS, Angnes L. Electrochemical immunosensors-A powerful tool for analytical applications. Biosens Bioelectron. 2018;102:470–78.
4. Matsunaga T, Kamiya S. Use of magnetic particles isolated from magnetotactic bacteria for enzyme immobilization. Appl Microbiol Biotechnol. 1987;26(4):328–32.
5. Bazylinski DA, Frankel RB. Magnetosome formation in prokaryotes. Nat Rev Microbiol. 2004;2(3):217–30.
6. Schüler D. The biomineralization of magnetosomes in Magnetospirillum gryphiswaldense. Int Microbiol. 2002;5(4):209–14.
7. Yan L, Da H, Zhang S, López VM, Wang W. Bacterial magnetosome and its potential application. Microbiol Res. 2017;203:19–28.
8. Gorby YA, Beveridge TJ, Blakemore RP. Characterization of the bacterial magnetosome membrane. J Bacteriol. 1988;170(2):834–41.
9. Grünberg K, Muller E-C, Otto A, Reszka R, Linder D, Kube M, et al. Biochemical and proteomic analysis of the magnetosome membrane in Magnetospirillum gryphiswaldense. Appl Environ Microbiol. 2004;70(2):1040–50.
10. Nakamura N, Hashimoto K, Matsunaga T. Immunoassay method for the determination of immunoglobulin G using bacterial magnetic particles. Anal Chem. 1991;63(3):268–72.
11. Sun JB, Duan JH, Dai SL, Ren J, Guo L, Jiang W, et al. Preparation and anti-tumor efficiency evaluation of doxorubicin-loaded bacterial magnetosomes: magnetic nanoparticles as drug carriers isolated from Magnetospirillum gryphiswaldense. Biotechnol Bioeng. 2008;101(6):1313–20.
12. Takeyama H, Tsuzuki H, Chow S, Nakayama H, Matsunaga T. Discrimination between Atlantic and Pacific subspecies of northern Bluefin tuna (Thunnus thynnus) by magnetic-capture hybridization using bacterial magnetic particles. Mar Biotechnol (NY). 2000;2(4):309–13.
13. Liu Y, Li GR, Guo FF, Jiang W, Li Y, Li J. Large-scale production of magnetosomes by chemostat culture of Magnetospirillum gryphiswaldense at high cell density. Microb Cell Factories. 2010;9:99.
14. Tanaka T, Matsunaga T. Fully automated chemiluminescence immunoassay of insulin using antibody−protein A−bacterial magnetic particle complexes. Anal Chem. 2000;72(15):3518–22.
15. Pečová M, Šebela M, Marková Z, Poláková K, Čuda J, Šafářová K, et al. Thermostable trypsin conjugates immobilized to biogenic magnetite show a high operational stability and remarkable reusability for protein digestion. Nanotechnology. 2013;24(12):125102.

16. Li A, Zhang H, Zhang X, Wang Q, Tian JS, Li Y, et al. Rapid separation and immunoassay for low levels of Salmonella in foods using magnetosome-antibody complex and real-time fluorescence quantitative PCR. J Sep Sci. 2010;33(21):3437–43.
17. Nakamura N, Burgess JG, Yagiuda K, Kudo S, Sakaguchi T, Matsunaga T. Detection and removal of Escherichia coli using fluorescein isothiocyanate conjugated monoclonal antibody immobilized on bacterial magnetic particles. Anal Chem. 1993;65(15):2036–39.
18. Nakamura N, Matsunaga T. Highly sensitive detection of allergen using bacterial magnetic particles. Anal Chim Acta. 1993;281(3): 585–89.
19. Matsunaga T, Ueki F, Obata K, Tajima H, Tanaka T, Takeyama H, et al. Fully automated immunoassay system of endocrine disrupting chemicals using monoclonal antibodies chemically conjugated to bacterial magnetic particles. Anal Chim Acta. 2003;475(1–2):75–83.
20. Gonzalez-Sapienza G, Rossotti MA, Tabares-da Rosa S. Single-domain antibodies as versatile affinity reagents for analytical and diagnostic applications. Front Immunol. 2017;8:977.
21. Shen M, Rusling J, Dixit CK. Site-selective orientated immobilization of antibodies and conjugates for immunodiagnostics development. Methods. 2017;116:95–11.
22. Trilling AK, Harmsen MM, Ruigrok VJ, Zuilhof H, Beekwilder J. The effect of uniform capture molecule orientation on biosensor sensitivity: dependence on analyte properties. Biosens Bioelectron. 2013;40(1):219–26.
23. Davenport KR, Smith CA, Hofstetter H, Horn JR, Hofstetter O. Site-directed immobilization of a genetically engineered anti-methotrexate antibody via an enzymatically introduced biotin label significantly increases the binding capacity of immunoaffinity columns. J Chromatogr B Anal Technol Biomed Life Sci. 2016;1021: 114–21.
24. Sukhanova A, Even-Desrumeaux K, Kisserli A, Tabary T, Reveil B, Millot JM, et al. Oriented conjugates of single-domain antibodies and quantum dots: toward a new generation of ultrasmall diagnostic nanoprobes. Nanomedicine. 2012;8(4):516–25.
25. Pollithy A, Romer T, Lang C, Müller FD, Helma J, Leonhardt H, et al. Magnetosome expression of functional camelid antibody fragments (nanobodies) in Magnetospirillum gryphiswaldense. Appl Environ Microbiol. 2011;77(17):6165–71.
26. Suzuki S, Hasegawa A. Determination of hexabromocyclododecane diastereoisomers and tetrabromobisphenol A in water and sediment by liquid chromatography/mass spectrometry. Anal Sci. 2006;22(3): 469–74.
27. Harrad S, Abdallah MAE, Rose NL, Turner SD, Davidson TA. Current-use brominated flame retardants in water, sediment, and fish from English lakes. Environ Sci Technol. 2009;43(24):9077–83.
28. Zhang Z, Zhu N, Huang M, Liang Y, Zeng K, Wu X, et al. Sensitive immunoassay for simultaneous determination of tetrabromobisphenol A bis(2-hydroxyethyl) ether and tetrabromobisphenol A mono(hydroxyethyl) ether: an effective and reliable strategy to estimate the typical tetrabromobisphenol A derivative and byproduct in aquatic environments. Environ Pollut. 2017;229:431–38.
29. Covaci A, Voorspoels S, Abdallah MAE, Geens T, Harrad S, Law RJ. Analytical and environmental aspects of the flame retardant tetrabromobisphenol-A and its derivatives. J Chromatogr A. 2009;1216(3):346–63.
30. Wang J, Bever CR, Majkova Z, Dechant JE, Yang J, Gee SJ, et al. Heterologous antigen selection of camelid heavy chain single domain antibodies against tetrabromobisphenol A. Anal Chem. 2014;86(16):8296–302.
31. Xu T, Wang J, Liu SZ, Lü C, Shelver WL, Li QX, et al. A highly sensitive and selective immunoassay for the detection of tetrabromobisphenol A in soil and sediment. Anal Chim Acta. 2012;751:119–27.
32. Schneider P, Hammock BD. Influence of the ELISA format and the hapten-enzyme conjugate on the sensitivity of an immunoassay for S-triazine herbicides using monoclonal antibodies. J Agric Food Chem. 1992;40(3):525–30.
33. Yang Y, Lu L, Zhang J, Yang Y, Wu Y, Shao B. Simultaneous determination of seven bisphenols in environmental water and solid samples by liquid chromatography-electrospray tandem mass spectrometry. J Chromatogr A. 2014;1328:26–34.
34. Heyen U, Schüler D. Growth and magnetosome formation by microaerophilic Magnetospirillum strains in an oxygen-controlled fermentor. Appl Microbiol Biotechnol. 2003;61(5–6):536–44.
35. Zhang Y, Zhang X, Jiang W, Li Y, Li J. Semicontinuous culture of Magnetospirillum gryphiswaldense MSR-1 cells in an autofermentor by nutrient-balanced and isosmotic feeding strategies. Appl Environ Microbiol. 2011;77(17):5851–56.
36. Yang J, Li S, Huang X, Tang T, Jiang W, Zhang T, et al. A key time point for cell growth and magnetosome synthesis of Magnetospirillum gryphiswaldense based on real-time analysis of physiological factor. Front Microbiol. 2013;4:210.
37. Wang J, Majkova Z, Bever CR, Yang J, Gee SJ, Li J, et al. One-step immunoassay for tetrabromobisphenol a using a camelid single domain antibody-alkaline phosphatase fusion protein. Anal Chem. 2015;87(9):4741–48.
38. Saerens D, Conrath K, Govaert J, Muyldermans S. Disulfide bond introduction for general stabilization of immunoglobulin heavy-chain variable domains. J Mol Biol. 2008;377(2):478–88.
39. Arya S, Wang KY, Wong CC, Rahman AR. Anti-EpCAM modified LC-SPDP monolayer on gold microelectrode based electrochemical biosensor for MCF-7 cells detection. Biosens Bioelectron. 2013;41:446–51.
40. Yoon TJ, Lee W, Oh YS, Lee JK. Magnetic nanoparticles as a catalyst vehicle for simple and easy recycling. New J Chem. 2003;27(2):227–29.
41. Yu T, Cheng W, Li Q, Luo C, Yan L, Zhang D, et al. Electrochemical immunosensor for competitive detection of neuron specific enolase using functional carbon nanotubes and gold nanoprobe. Talanta. 2012;93:433–38.
42. Abdallah MA-E. Environmental occurrence, analysis and human exposure to the flame retardant tetrabromobisphenol-A (TBBP-A)—a review. Environ Int. 2016;94:235–50.